Engineering Failure Analysis 163 (2024) 108439

Contents lists available at ScienceDirect

Engineering Failure Analysis

journal homepage: www.elsevier.com/locate/engfailanal

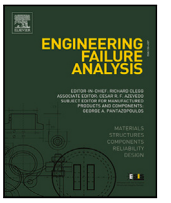

Comparative study on bending behavior and damage analysis of 3D-printed sandwich core designs with bio-inspired reinforcements

M. Gokhan Atahan *, Merve Erikli, Enes Ozipek, Fulya Ozgun

Department of Mechanical Engineering, Abdullah Gul University, Kayseri, Turkiye

ARTICLE INFO

Keywords:
Additive manufacturing
Bio-inspired design
Sandwich core
Bending behavior
Sandwich structure

ABSTRACT

In this study, novel sandwich core designs with bio-inspired reinforcements were proposed and their bending behaviors were comparatively examined. The geometrical shapes of alligator osteoderm and chambered nautilus shell were utilized as bio-inspired reinforcements for sandwich core structures. Sandwich core structures were produced through the additive manufacturing method. Experimental tests and finite element analysis were performed to determine the bending performances of the proposed sandwich core structures. The load-carrying capacity, deformation ability, damage-tolerant capability, energy absorption, and damage mechanisms of the proposed sandwich core structures were comparatively investigated through experimental and numerical methods. The orthotropic material model and Hashin's damage criterion were used in the numerical model of 3D-printed sandwich core structures to consider the effect of the filament raster orientation on the elastic and damage behavior of the sandwich core structures. Compared to the classical honeycomb sandwich core structure, while bio-inspired reinforcements improved the load-carrying capacity and damage-tolerant capability of sandwich core structures, they reduced the energy absorption ability of sandwich core structures due to reducing the vertical deformation ability of sandwich core structures. Bio-inspired reinforcements significantly affected the stress distribution and damage behavior of the sandwich core structures. They reduced von Mises stress level at the outer cell edges of the sandwich core structures and caused reinforcement damage instead of outer cell damage.

1. Introduction

Sandwich structures consist of top and bottom face sheets and a core structure, and are obtained by bonding the face sheets onto the core structure [1–3]. Sandwich structures are widely used as crashworthiness structures in many industrial sectors such as automotive, aerospace, and military due to their high strength-to-weight ratio, good thermal insulation, and excellent energy absorption capability [3–6]. Sandwich core structures are exposed to tensile, compressive, and shear stresses under bending load. The combined stress state occurs in sandwich core structures and this affects the damage initiation and propagation stages. Hence, numerous researchers have investigated the bending response of sandwich structures [2,4,7].

The mechanical properties of the sandwich structure are highly dependent on the geometry of the core structure. Therefore, the mechanical properties of the sandwich structure can be improved by designing the new core geometry [4]. Honeycomb sandwich core structure has been widely used in engineering applications for a long time. However, traditional honeycombs have some problems such as low compressive strength, relatively poor impact resistance, production time, and production quality inconsistencies. These problems have led researchers to develop new sandwich core structures [8]. The emergence of additive

* Corresponding author.
E-mail address: mithatgokhan.atahan@agu.edu.tr (M.G. Atahan).

https://doi.org/10.1016/j.engfailanal.2024.108439
Received 27 March 2024; Received in revised form 30 April 2024; Accepted 12 May 2024
Available online 22 May 2024

manufacturing (3D printing) provides design freedom, and thus novel sandwich core structures have been produced in order to replace the traditional honeycomb core structure [5,9–12]. 3D printing is based on a manufacturing system that involves deposition layer by layer. Since 3D printing provides the opportunity to produce complex shapes, its use in industrial applications has increased [9]. Lu et al. [13] designed Bi-Grid, Tri-Grid, Quadri-Grid, and Kagome-Grid honeycombs and produced them using a 3D-printer. They reported that the Quadri-Grid sandwich structure showed better mechanical performance compared to other sandwich structures. Li and Wang [14] compared the bending behavior of sandwich structures with 3D-printed truss, conventional honeycomb, and re-entrant honeycomb core structures. They stated that compared to the re-entrant honeycomb sandwich structure, the truss and conventional honeycomb sandwich structures exhibited catastrophic failure earlier because of the localized stress concentration. Chahardoli [9] investigated the bending behavior of 3D-printed sandwich structures with cellular cores using trapezoidal geometries. Rangapuram et al. [8] determined that there was an enhancement in the mechanical performance of additively manufactured modified honeycomb cores because of the increased bonding surface area. Geramizadeh et al. [15] proposed novel Beta VI and Alpha VI core structures produced with 3D printing in order to improve the energy absorption capacity of the honeycomb sandwich beam. Pirouzfar and Zeinedini [16] revealed that the flexural properties of the sandwich structure with a honeycomb core were significantly improved by replacing the core material from Nomex to 3D-printed PLA (Polylactic acid). Haldar et al. [11] proposed a corrugated core design produced with 3D printing in order to improve the compressive properties of the sandwich structure. Indreş et al. [10] investigated the effect of the different core topologies on the bending behavior of 3D-printed sandwich beams. They found that when the relative density was higher and the re-entrant cell was placed at 90°, the specific absorbed energy capability was improved compared to the honeycomb core. Geramizadeh et al. [17] compared the bending performance of 3D-printed hexagonal honeycomb and re-entrant honeycomb sandwich beams. Eryildiz [18] investigated the flexural properties of the 3D-printed new sandwich core designs. It was reported that the maximum bending strength of sandwich structures with triple-core topology was higher than that of single-core topology. Zhang et al. [19] proposed a 3D-printed variable-density core design in order to improve the bending strength, bending stiffness, shear strength, and energy absorption capability of the sandwich structures.

Since biological systems have been optimized by nature over millions of years, bio-inspired structures are expected to provide good functional properties [12]. Nature offers good examples of designing new sandwich core structures with excellent mechanical properties [20,21]. In recent years, researchers have focused on bio-inspired sandwich core structures, thus providing significant improvements in the mechanical properties of sandwich structures. There are many studies in the literature that improve the impact behavior of sandwich structures with a novel bio-inspired core [22] (e.g., woodpecker's head configuration-inspired [23], bamboo-spiderweb-inspired hybrid cellular structure [21,24], the microstructure of a woodpecker's beak-inspired [20], the local geometric configuration of the glass sponge-inspired [25]). Sandwich structures are expected to improve their energy absorption capabilities under dynamic loads as well as high mechanical performance under quasi-static loads such as compression, shear, and bending. Bru et al. [12] compared the compressive and flexural properties of honeycomb, enamel-inspired, and bamboo-inspired core configurations produced by 3D printing. They stated that the proposed bio-inspired core structures were potential competitors to the traditional honeycomb core structure in terms of strength, stiffness, and energy absorption. Yu et al. [26] modified the honeycomb structure considering the microstructure of beetle elytra in order to improve the energy absorption ability of the crash boxes. Chouhan et al. [27] developed three bio-inspired structures (centriole, nautilus, and cartwheel) and produced them with SLA (Stereolithography) 3D printing. They found that the cartwheel structure was stiffer and stronger than other bio-inspired structures with nearly the same volume. Bhat et al. [28] developed architectured materials with interlocking designs inspired by the atomic arrangements in cubic metallic crystal structures. They produce the biomimetic structures with HP-MJF 4200 powder bed fusion technology. They stated that the combination of novel structures can be used as an effective solution to meet complex multi-functional requirements in printed products. Doodi and Gunji [29] investigated experimentally and numerically the mechanical performance of novel hybrid bio-inspired (the bamboo tree, fish scales, and scutes observed from crocodile skin) 3D-printed lattice structures in terms of stiffness and energy absorption capability. Peng et al. [30] carried out a three-point bending test on the 3D-printed bio-inspired sandwich beam designs, and their result showed that sandwich structures with a Neovius core showed better mechanical performance compared to other core designs. Song et al. [31] proposed a hierarchical honeycomb metastructure design method depending on conformal criteria and improved the energy absorption capability of the honeycomb core structures. Ullah et al. [32] evaluated the mechanical performance of the bio-inspired Kagome truss core structures under compression and shear loading and determined that both the compression and shear performance of the bio-inspired core produced by additive manufacturing were superior (strength) or equal (hardness) compared to honeycomb cores for aerospace applications. Hu et al. [33] presented biomimetic cellular structural composite designs such as the 2D honeycomb hexagon model, 2D cuttlefish model, and 3D octahedron model in order to achieve an ultra-lightweight and high-strength structure. Nian et al. [34] proposed bio-inspired graded honeycomb filler designs to enhance the energy absorption capability. Zhang et al. [35] investigated the crashworthiness characteristic of the bio-inspired self-similar regular hierarchical honeycombs. Yang et al. [36] examined the collapse behavior of the sandwich panel with the bio-inspired bi-directionally corrugated core under out-of-plane crushing load. They found that the bio-inspired double-sine corrugated sandwich structure greatly improved the energy absorption capacity and reduced the initial peak force greatly compared to regular triangular, sinusoidal corrugated core sandwich panels. Song et al. [37] investigated the failure mechanism of novel additively manufactured bio-inspired elytra-like interlocked sandwich structures under compression and bending loads and determined the optimal design dimensions.

It is shown that numerous researchers have improved the mechanical performance of sandwich structures with bio-inspired sandwich core designs. Due to the development of the additive manufacturing method, studies in this field have increased recently. However, studies on the development of new sandwich structures are still limited. The main novelty of this work lies in the design of novel 3D-printed sandwich cores with bio-inspired reinforcements. The aim of this research is to compare the bending behavior

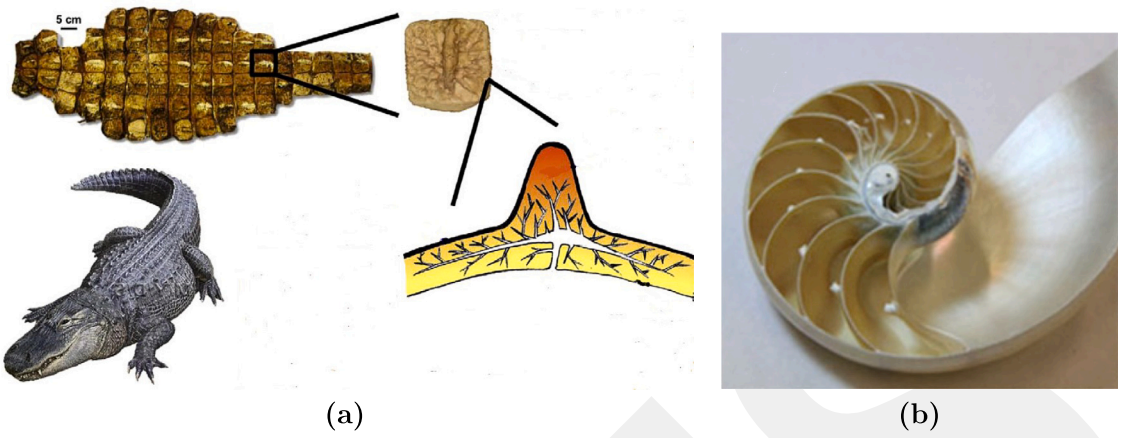

Fig. 1. Geometrical shapes of (a) alligator osteoderm (reprinted with permission from Elsevier [38]) and (b) chambered nautilus shell (reprinted with permission from the Royal Society Publishing [39]).

of 3D-printed sandwich core designs with bio-inspired reinforcement in terms of maximum load, maximum deflection, flexural stiffness, and absorbed energy. Reinforcements for sandwich core structures were designed according to the geometrical structure of alligator osteoderm and chambered nautilus shell. A total of 10 sandwich core designs were considered in this study, three without reinforcement, three with alligator osteoderm reinforcement, and four with chambered nautilus shell reinforcement. A 3D-finite element analysis was performed to determine the damage types of the sandwich core structures.

2. Experimental study

2.1. Sandwich core design

The main aim of this study is to compare the bending characteristics of sandwich core structures with bio-inspired reinforcements. The geometrical shapes of alligator osteoderm and chambered nautilus shell are presented in Fig. 1. In this study, ten types of sandwich cores were designed with Solidworks design software as shown in Fig. 2, which can be categorized into three groups: sandwich core designs with non-reinforcement, sandwich core designs with alligator osteoderm-inspired reinforcement, sandwich core designs with chambered nautilus shell-inspired reinforcement. Non-reinforced core structures were inspired by honeycomb, alligator osteoderm, and chambered nautilus shell outer frame structures. The reinforcement structures of the sandwich cores were designed considering alligator osteoderm and chambered nautilus shell inner structure. Alligator osteoderm has high resistance to external loads and was used as armor clothes for ancient warriors [38,40]. The nautilus is a species that lives in deep coastal water and has spirally coiled internal structures. The spiral internal structure increases its resistance to hydrostatic pressure under deep water [27]. The geometries of both the outer cells (square (alligator osteoderm) and circular (chambered nautilus shell)) and internal reinforcements of the alligator osteoderm and chambered nautilus shell structures were taken into consideration. In addition, these bio-inspired reinforcements were placed inside the traditional honeycomb sandwich core structure and their effect on the bending behavior of the sandwich structure was examined. As seen in Fig. 1, there is a conical reinforcement in the alligator osteoderm structure and this structure provides high durability under compressive and bending loads [38,40]. Similarly, the chambered nautilus shell structure shows high mechanical performance under hydrostatic pressure (compression) [27]. As a result, the geometrical structures of the alligator osteoderm and the chambered nautilus shell were adapted to sandwich core structures because of their superior mechanical properties under compression and bending loads. The dimensions of the sandwich core structures are shown in Fig. 3. The outer frames of sandwich core structures were designed in hexagonal (honeycomb), square (alligator osteoderm), and circular (chambered nautilus shell) shapes. For all sandwich core designs, the outer frame wall thickness is 1.4 mm. Similarly, the wall thickness of the chambered nautilus shell-inspired internal reinforcements was considered as 1.4 mm. However, there is a conical internal reinforcement in the alligator osteoderm structure (Fig. 1a). For this reason, the alligator osteoderm-inspired internal reinforcements were designed in a conical shape and the reinforcement thickness varies between 1 and 1.4 mm (Fig. 3). The chambered nautilus shell-inspired reinforcements were placed to contact the corners of the outer frame of the hexagonal and square shapes (Designs 7 and 8). The internal reinforcements of Designs 9 and 10 were designed with reference to Designs 7 and 8, respectively, for comparison. The overall dimensions of sandwich core structures with honeycomb, square, and circular outer frames were set as 132 × 56 × 10, 146 × 63 × 10, and 149 × 65 × 10 mm, respectively to provide the same number of cells (7 × 3).

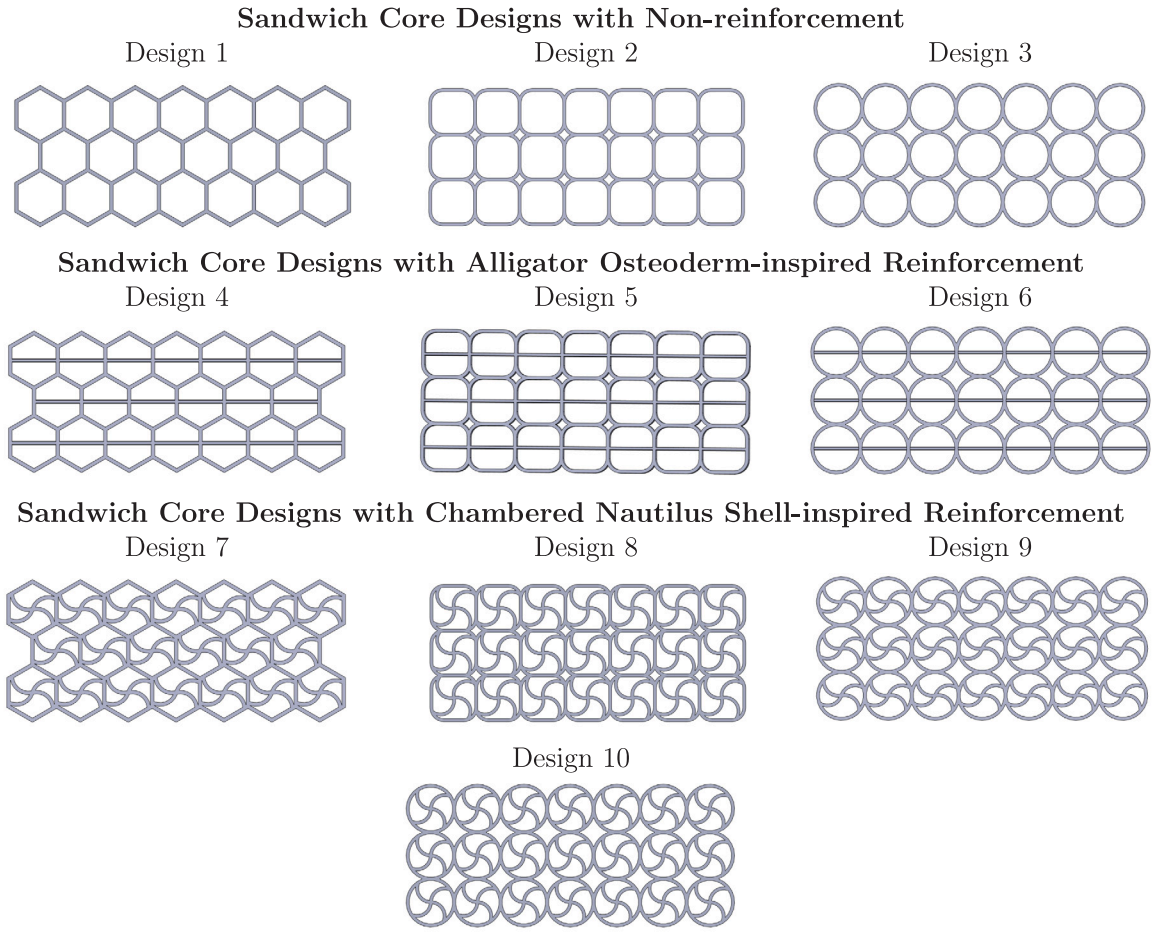

Fig. 2. Non-reinforced and reinforced sandwich core designs.

Table 1
Printing parameters of sandwich core designs.

Printer type	Ultimaker 2+
Material	Polylactic acid (PLA)
Printing temperature	210 °C
Build plate temperature	60 °C
Nozzle diameter	0.4 mm
Layer height	0.1 mm
Printing speed	50 mm/s
Infill pattern	Lines
Infill line direction	0°
Infill density	100%

2.2. Manufacturing of sandwich core designs

After the design of the sandwich core structures, the part models were converted to the STL (Stereolithography) file using Solidworks design software. Then, G-codes, manufacturing codes, were generated using Ultimaker Cura software. The fused deposition modeling method (FDM) was preferred to produce sandwich core structures [16]. Filaments were laid with 0° to carry effectively the bending load (Fig. 4a). Sandwich core designs were fabricated using an Ultimaker 2 + 3D printer (Fig. 4b). The printing parameters of sandwich core designs are presented in Table 1. Ultimaker polylactic acid (PLA) filament with a diameter of 2.85 mm was used to produce the sandwich core structures. Printed sandwich core structures were weighed with a precision electronic balance to normalize the bending test results, and measured weight values of sandwich core designs are presented in Table 2.

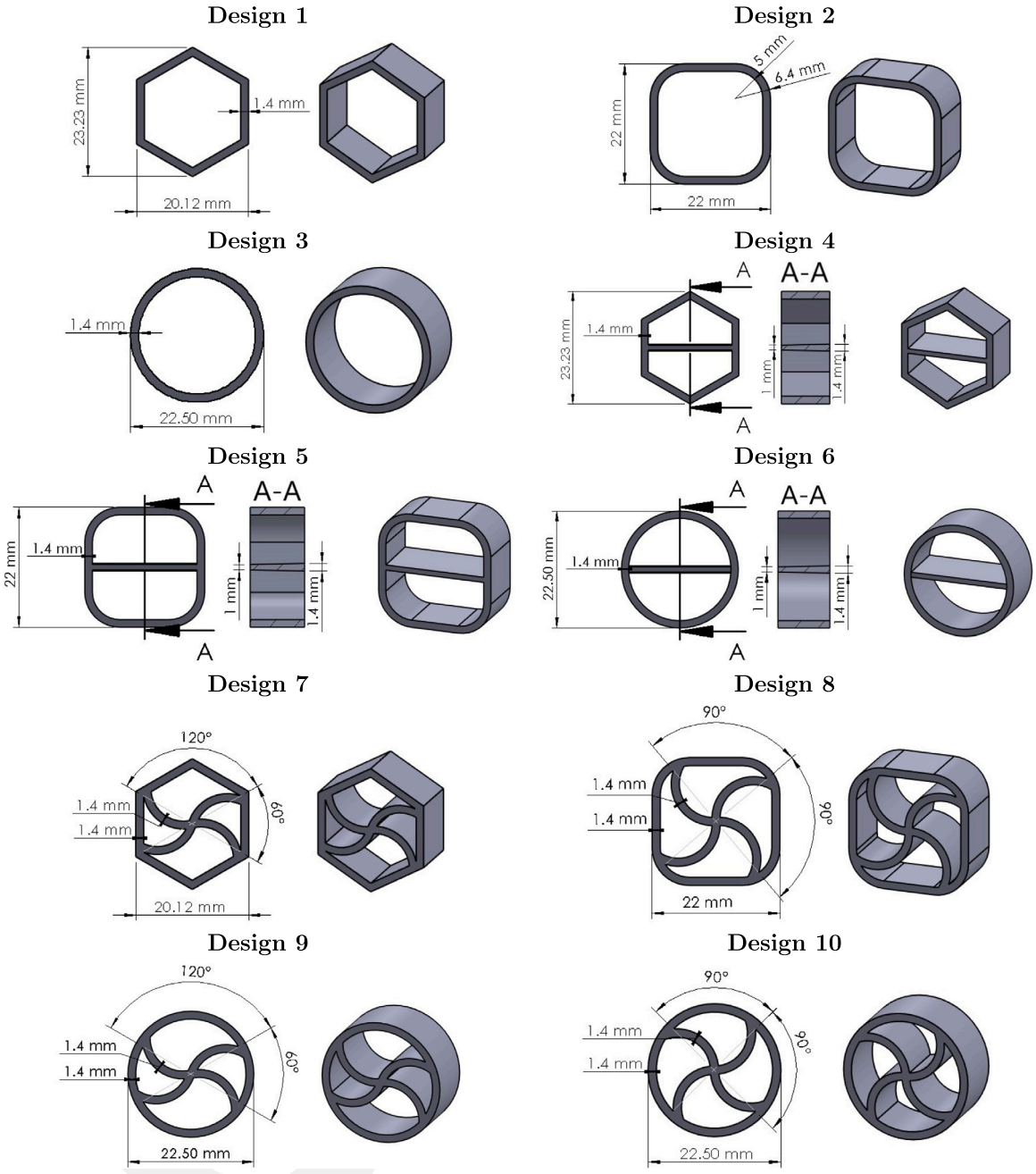

Fig. 3. Dimensions of sandwich core designs.

2.3. Three-point bending test

Three-point bending tests were performed at room temperature using a Shimadzu universal test machine with a constant cross-head speed of 2 mm/min (Fig. 4c). Bru et al. [12] carried out the bending test of bio-inspired sandwich core structures according to the ASTM C393 test standard. Using a similar approach, the ASTM C393 test standard [41] was used to determine the bending behavior of the sandwich core structures. The support span length was set as 80 mm. The diameter of all supports was selected as 10 mm. At least three repeated tests were carried out for each sandwich core structure. A bending load was applied to the sandwich core structures up to specimen failure. Then, the force and deflection values of each sandwich core structure were obtained. The load–deflection variable is used to characterize the bending behavior of sandwich core structures.

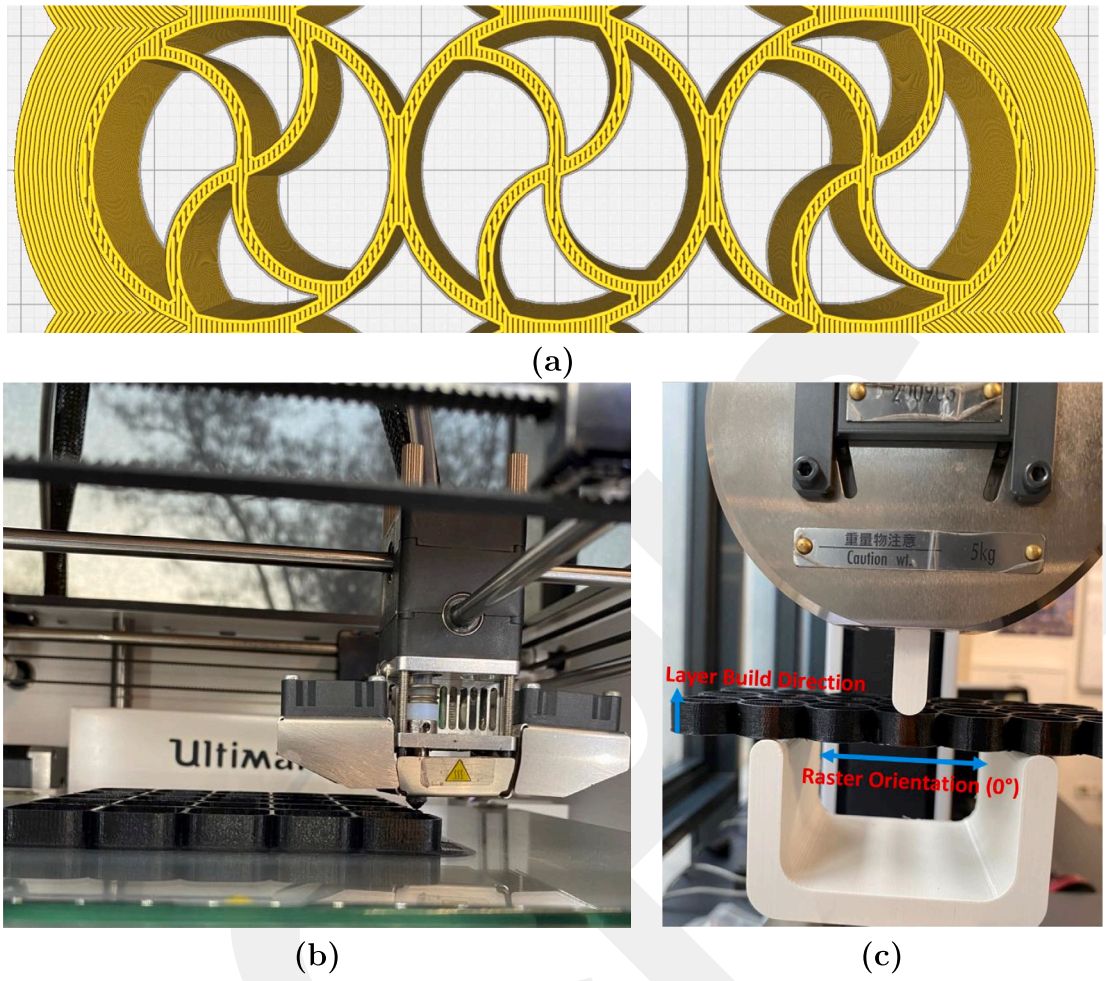

Fig. 4. Demonstration of (a) infill line direction, (b) fabrication, and (c) bending test configuration of sandwich core designs.

Table 2
Measured weight values of sandwich core designs.

	Weight (g)	Standard deviation
Design 1	11.27	0.47
Design 2	14.87	0.71
Design 3	16.98	0.54
Design 4	15.01	0.82
Design 5	19.07	0.82
Design 6	22.07	0.62
Design 7	23.67	0.41
Design 8	31.76	0.18
Design 9	30.16	0.59
Design 10	29.90	0.11

A typical load–deflection curve of the sandwich core structure subject to bending load is shown in Fig. 5 [5]. Part I is called the elastic region that relates to the damage-tolerant capability. In this region, sandwich core structures have a linear behavior. In order to evaluate the damage-tolerant performance of sandwich core structures, flexural stiffness was determined considering the slope of the elastic curve. Part II covers the damage initiation and propagation stages. Since damage initiates in this region, non-linear behavior is observed. The bending load increases until final failure occurs and finally it is abruptly dropped. The maximum load and largest deflection values of the sandwich core structures are obtained from this point where the failure occurs. Finally, the area under the load–deflection curve is equal to the amount of absorbed energy by the sandwich core structures [5]. In order to compare the mechanical properties of sandwich structures, the mechanical test results were normalized using the weight values of sandwich structures in many studies [16,42,43]. In this study, bending test results were normalized using the weight values of

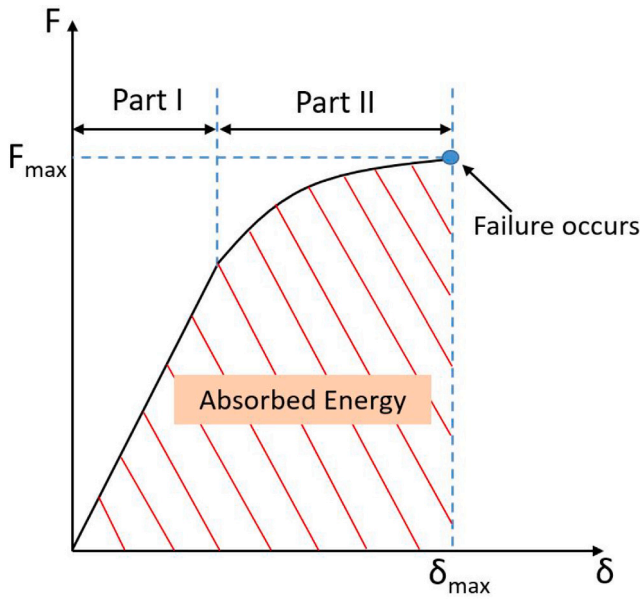

Fig. 5. Typical load–deflection (F-δ) curve of the sandwich core structure subject to bending load.

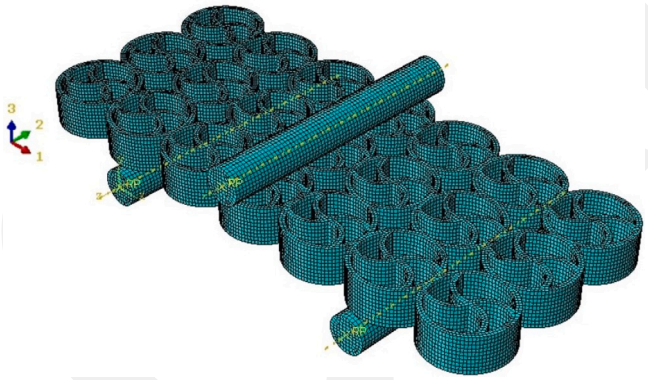

Fig. 6. Finite element model of the sandwich core design.

sandwich core structures, and the effect of bio-inspired reinforcements on the bending behavior of sandwich core structures was examined comparatively.

3. Numerical model

In order to determine the damage type and stress distribution of the sandwich core designs, three-dimensional finite element analyses were performed using ABAQUS/Standard software. The finite element model of sandwich core structures is demonstrated in Fig. 6. The loading part and bottom supports were modeled as discrete rigid and meshed using an R3D4 element type while the SC8R element type was used for sandwich core structures. Linear and rotational movements of the bottom supports were prevented in all axes, namely all degrees of freedom of the bottom supports were fixed at zero. The loading part can move only along the y-direction. The sandwich core structures were bent by applying displacement to the middle region of the specimen along the negative y-axis direction. The contact behavior was considered by implementing a surface-to-surface contact algorithm with tangential behavior in the numerical model. A coefficient of friction was defined as 0.2 between the contacting surfaces.

Mesh sensitivity analysis was performed with preliminary analyses considering a variety of element sizes (1.2–0.6 mm) for all sandwich core structures and was evaluated according to the variation in the maximum force value of the sandwich core structures. The element size was selected as 0.8 mm for all sandwich core structures considering results consistency and saving the calculation time. The mechanical properties of the 3D-printed part vary depending on the filament raster direction. Therefore, the orthotropic material model approach was assumed in the numerical modeling of the 3D-printed specimen [44–46]. In this study, 3D-printed

Table 3
Mechanical properties of 3D-printed PLA.

Property	Symbol	Unit	Value
Longitudinal modulus of elasticity [44]	E_1	MPa	3015.25
Transverse modulus of elasticity [44]	E_2	MPa	2659.05
Transverse modulus of elasticity [44]	E_3	MPa	2054.90
Shear modulus [46]	$G_{12} = G_{13}$	MPa	817
Shear modulus	G_{23}	MPa	984.83
Poisson's ratio [46]	$\upsilon_{12} = \upsilon_{13} = \upsilon_{23}$		0.35
Longitudinal tensile strength [52]	X^T	MPa	42
Transverse tensile strength [52]	Y^T	MPa	27.59
Longitudinal compressive strength [53]	X^C	MPa	78.54
Transverse compressive strength [53]	Y^C	MPa	79.83
In-plane shear strength [45]	$S_{12} = S_{13}$	MPa	30.61
Interlaminar shear strength	S_{23}	MPa	39.91
Longitudinal tensile fracture energy [46,54]	G^c_{ft}	N/mm	18
Longitudinal compressive fracture energy [46,54]	G^c_{fc}	N/mm	18
Transverse tensile fracture energy [46,54]	G^c_{mt}	N/mm	4
Transverse compressive fracture energy [46,54]	G^c_{mc}	N/mm	4

sandwich core structures were modeled as an elastic orthotropic material using a similar approach. The orthotropic material model and damage estimation in ABAQUS® [47] are carried out using formulations developed by Matzenmiller et al. [48], Hashin and Rotem [49], Hashin [50], and Camanho and Davila [51]. Stress–strain (σ-ε) relations of the orthotropic material model are presented as follows in matrix form.

$$\begin{bmatrix}\sigma_{11}\\ \sigma_{22}\\ \sigma_{33}\\ \sigma_{12}\\ \sigma_{13}\\ \sigma_{23}\end{bmatrix} = \begin{bmatrix} D_{1111} & D_{1122} & D_{1133} & 0 & 0 & 0 \\ & D_{2222} & D_{2233} & 0 & 0 & 0 \\ & & D_{3333} & 0 & 0 & 0 \\ & & & D_{1212} & 0 & 0 \\ & symmetric & & & D_{1313} & 0 \\ & & & & & D_{2323} \end{bmatrix} \begin{bmatrix}\varepsilon_{11}\\ \varepsilon_{22}\\ \varepsilon_{33}\\ \gamma_{12}\\ \gamma_{13}\\ \gamma_{23}\end{bmatrix} \tag{1}$$

$$\begin{aligned} D_{1111} &= E_1(1-\upsilon_{23}\upsilon_{32})\Delta \\ D_{2222} &= E_2(1-\upsilon_{13}\upsilon_{31})\Delta \\ D_{3333} &= E_3(1-\upsilon_{12}\upsilon_{21})\Delta \\ D_{1122} &= E_1(\upsilon_{21}+\upsilon_{31}\upsilon_{23})\Delta = E_2(\upsilon_{12}+\upsilon_{32}\upsilon_{13})\Delta \\ D_{1133} &= E_1(\upsilon_{31}+\upsilon_{21}\upsilon_{32})\Delta = E_3(\upsilon_{13}+\upsilon_{12}\upsilon_{23})\Delta \\ D_{2233} &= E_2(\upsilon_{32}+\upsilon_{12}\upsilon_{31})\Delta = E_3(\upsilon_{23}+\upsilon_{21}\upsilon_{13})\Delta \\ D_{1212} &= G_{12} \\ D_{1313} &= G_{13} \\ D_{2323} &= G_{23} \end{aligned} \tag{2}$$

$$\Delta = \frac{1}{1-\upsilon_{12}\upsilon_{21}-\upsilon_{23}\upsilon_{32}-\upsilon_{31}\upsilon_{13}-2\upsilon_{21}\upsilon_{32}\upsilon_{13}} \tag{3}$$

Sabik et al. [46] utilized the Hashin's damage criterion in the damage analysis of 3D-printed PLA parts, and the developed numerical model was able to predict the damage behavior of 3D-printed structures well. Therefore, damage analysis of sandwich core structures was carried out according to Hashin's damage criterion. In this way, damage analysis of 3D-printed sandwich core structures was performed in terms of tension, compression, and shear damage types. Hashin damage model contains four main damage mechanisms: Tension failure mode in direction 1, Compression failure mode in direction 1, Tension failure mode in direction 2, and Compression failure mode in direction 2 [47,49]. Namely,

Tension failure mode in direction 1 ($\hat{\sigma}_{11} \geq 0$):

$$F_1^t = \left(\frac{\hat{\sigma}_{11}}{X^T}\right)^2 + \alpha\left(\frac{\hat{\tau}_{12}}{S^L}\right)^2 \tag{4}$$

Compression failure mode in direction 1 ($\hat{\sigma}_{11} < 0$):

$$F_1^c = \left(\frac{\hat{\sigma}_{11}}{X^C}\right)^2 \tag{5}$$

Tension failure mode in direction 2 ($\hat{\sigma}_{22} \geq 0$):

$$F_2^t = \left(\frac{\hat{\sigma}_{22}}{Y^T}\right)^2 + \left(\frac{\hat{\tau}_{12}}{S^L}\right)^2 \tag{6}$$

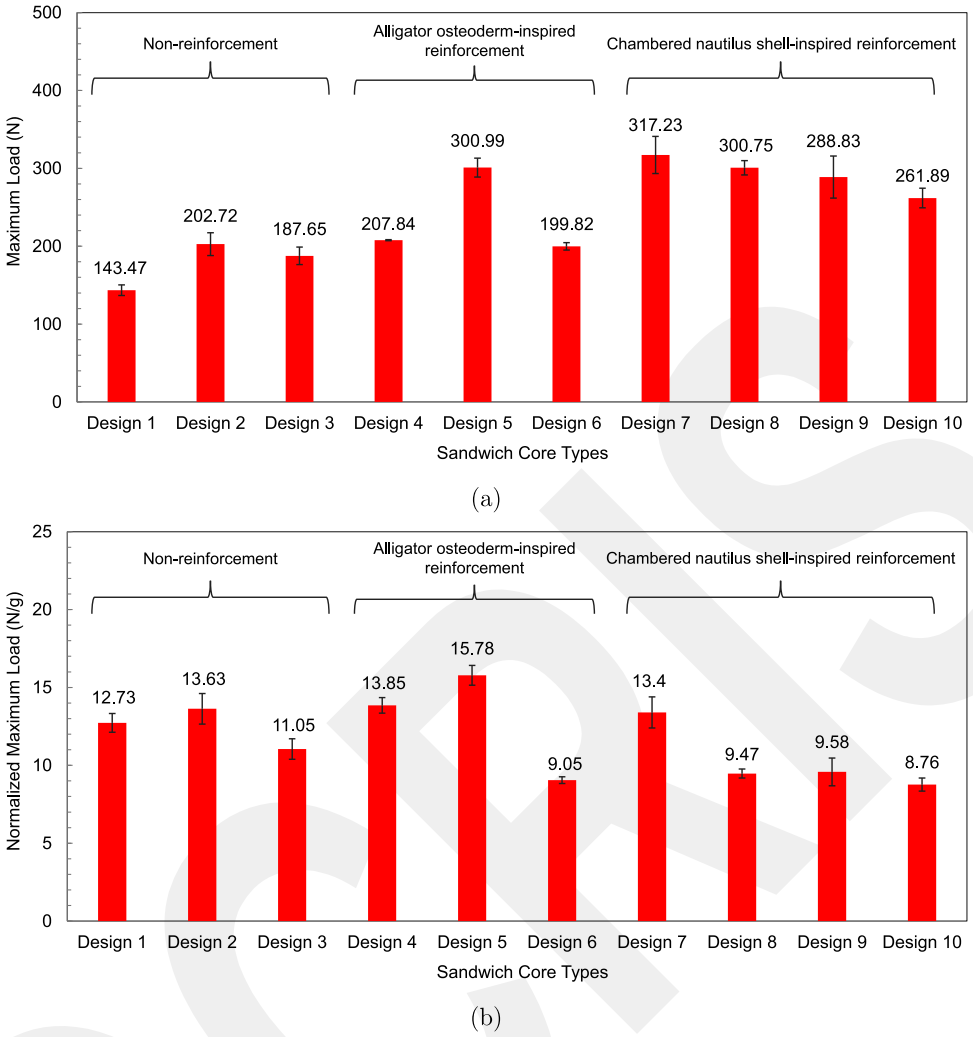

Fig. 7. Comparison of (a) measured and (b) normalized maximum load for different sandwich core types.

Compression failure mode in direction 2 ($\hat{\sigma}_{22} < 0$):

$$F_2^c = \left(\frac{\hat{\sigma}_{22}}{2S^T}\right)^2 + \left[\left(\frac{Y^C}{2S^T}\right)^2 - 1\right]\frac{\hat{\sigma}_{22}}{Y^C} + \left(\frac{\hat{\tau}_{12}}{S^L}\right)^2 \tag{7}$$

In the formulas above, X^T, X^C, Y^T, Y^C, S^L, and S^T denote longitudinal (direction 1) tensile strength, longitudinal (direction 1) compressive strength, transverse (direction 2) tensile strength, transverse (direction 2) compressive strength, in-plane shear strength, and transverse shear strength, respectively. In this study, the filament raster orientation of the 3D-printed sandwich core was evaluated as direction 1 and the perpendicular direction of the raster orientation was used as direction 2 (Figs. 4 and 6) [46]. The material properties used in the numerical model of 3D-printed sandwich core structures are presented in Table 3. Out-of-plane shear modulus and shear strength were determined by the following formulas [46,47].

$$G_{23} = \frac{E_2}{2(1+\upsilon_{23})} \tag{8}$$

$$S^T = \frac{Y^C}{2} \tag{9}$$

In the numerical model, the elastic behavior of 3D-printed sandwich core structures was examined with an orthotropic material model. However, the damage analysis was evaluated according to 2D-Hashin's damage criterion and therefore the damage throughout the thickness of the sandwich core structure was not taken into account. In this study, it was aimed to examine the effects of the novel sandwich core geometries on the damage behavior of the sandwich core structure. Namely, in-plane damage analysis (2D) is sufficient to observe the types of damage occurring in novel sandwich core geometries. Therefore, in-plane numerical

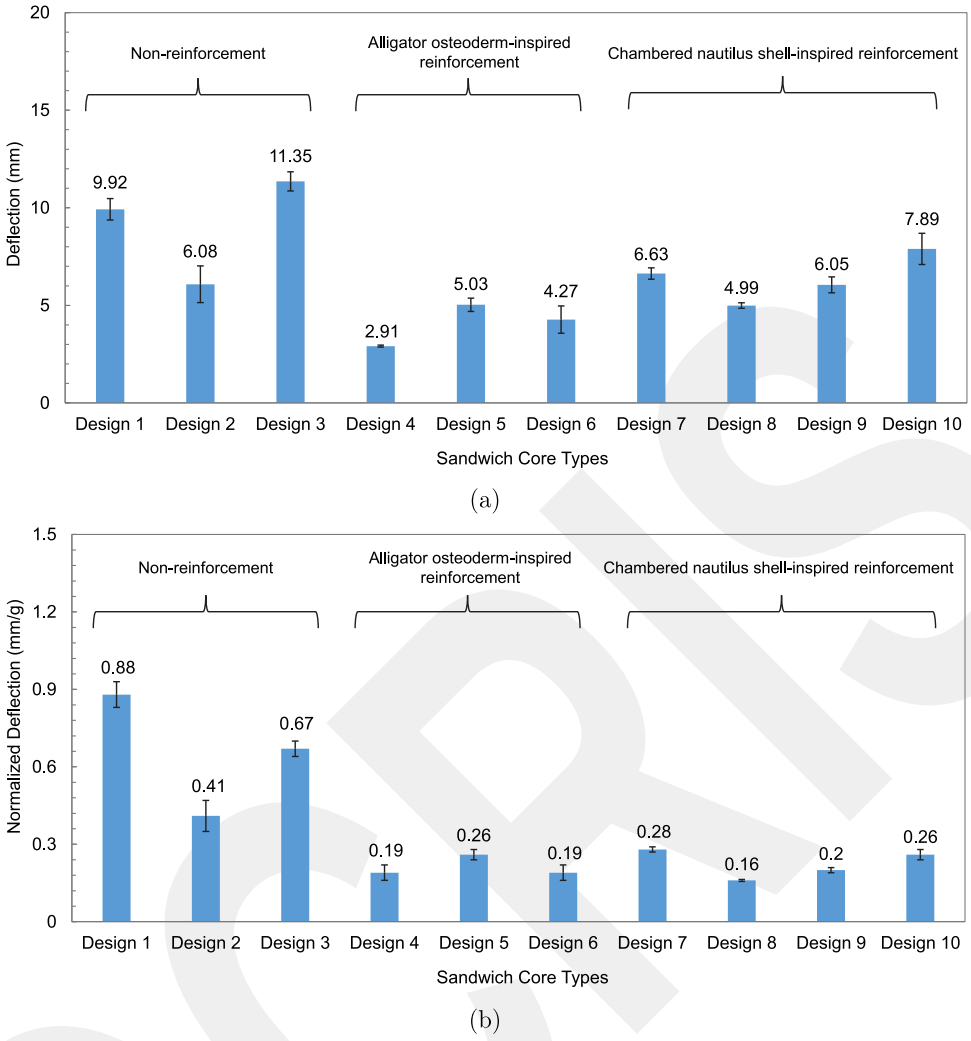

Fig. 8. Comparison of (a) measured and (b) normalized deflection for different sandwich core types.

damage images and damage types were presented using Hashin's damage criterion in the damage analysis. In this way, the effects of bio-inspired reinforcements on the damage behavior of sandwich core structures could be observed and the numerical in-plane damage analysis provided an important aspect in the damage mechanism of sandwich structures under bending load.

4. Results and discussion

The mechanical performances of 3D-printed sandwich core designs with bio-inspired reinforcement under bending load were compared according to load carrying capacity, largest deflection, flexural stiffness, and absorbed energy. The measured bending test results were normalized according to the weight of the sandwich core designs. In order to examine the effect of bio-inspired reinforcement on the bending behavior of sandwich core structures, the same outer cell designs were considered to compare the bending test results. That is, hexagonal outer cell designs (Designs 1, 4, 7), square outer cell designs (Designs 2, 5, 8), and circular outer cell designs (Designs 3, 6, 9, and 10) were compared with each other.

4.1. Comparison of maximum load

Measured maximum load values and normalized results of sandwich core designs are shown comparatively in Fig. 7. Considering non-reinforced sandwich core structures (Designs 1, 2, 3), Design 2 had the highest load-carrying capacity. The square outer cell design carried approximately 41.3% more bending load than the hexagonal cell design. Considering the effect of reinforcement type on the load-carrying capacity of sandwich core structures with the hexagonal outer cell (Designs 1, 4,7), according to the normalized results, alligator osteoderm-inspired reinforcement increased the load-carrying capacity of the sandwich core structure more than

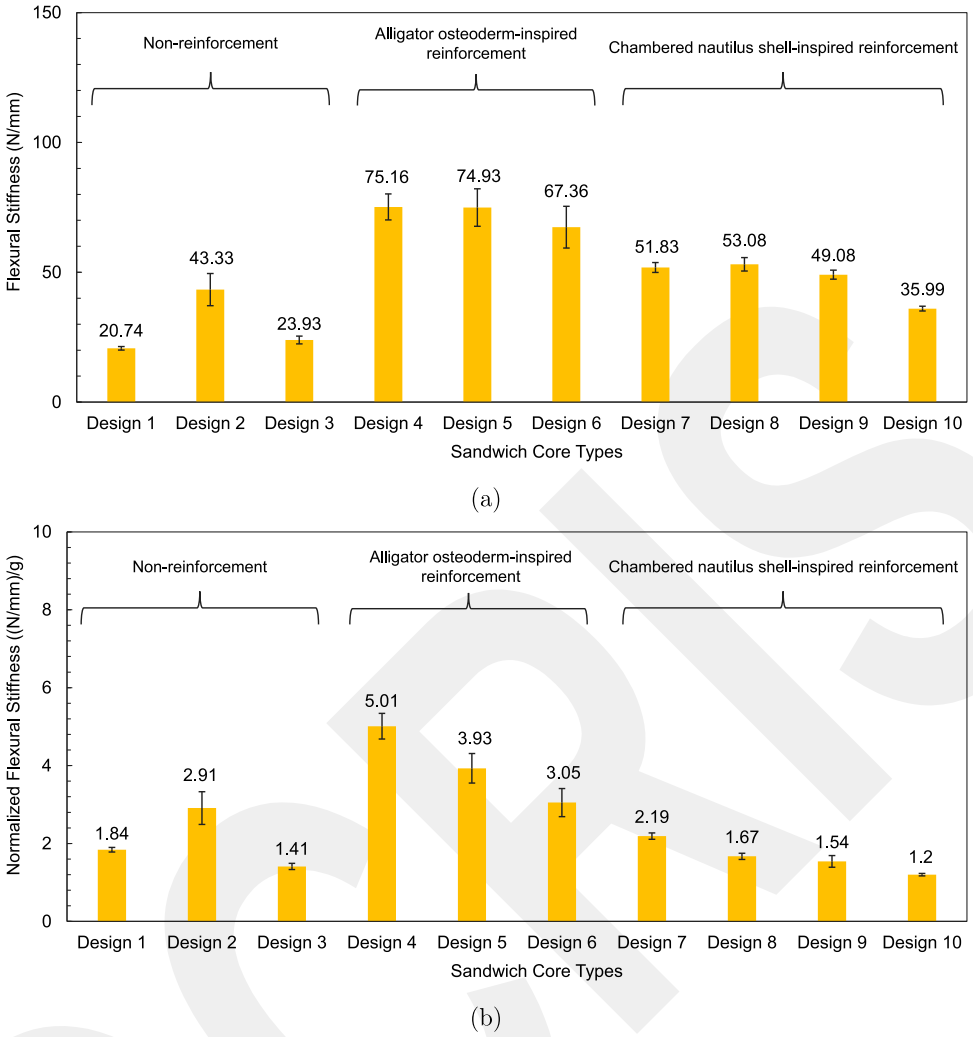

Fig. 9. Comparison of (a) measured and (b) normalized flexural stiffness for different sandwich core types.

chambered nautilus shell-inspired reinforcement. Similar results were also observed in sandwich core structures with the square outer cell (Designs 2, 5, 8). However, considering sandwich core structures with the circular outer cell, alligator osteoderm-inspired and chambered nautilus shell-inspired reinforcements decreased the load-carrying capacity of sandwich core structures (Designs 3, 6, 9, and 10). According to the measured maximum load values, although both reinforcement types increase the load-carrying capacity of sandwich core structures, the increase in weight is greater than the increase in load-carrying capacity, and therefore the load-carrying capacity of reinforced circular outer cell sandwich core structures is less than that of non-reinforced structures considering per unit weight. As a result, when both the outer cell and reinforcement designs of the sandwich core structures under the bending load were positioned perpendicular to the direction of the bending load, the load-carrying capacity of the sandwich core structure increased. Therefore, Design 5 had the highest load carrying capacity according to normalized results. Considering the test results of Design 9 and 10 using different chambered nautilus shell-inspired reinforcement angles, Design 9 had a higher load-carrying capacity than Design 10. Hence, it was observed that the angle between the reinforcement wings affects the bending load-carrying capacity of the sandwich core structure.

4.2. Comparison of maximum deflection

The vertical deformation capability of sandwich structures significantly affects the energy absorption capacity under bending load. Hence, the effects of bio-inspired reinforcement types on the deflection value of sandwich core structures under bending load were investigated. Fig. 8 indicates the measured and normalized deflection values at maximum load. While Design 3 had the maximum measured deflection value, the minimum deflection value was obtained from Design 4. Considering the normalized results, it was observed that the non-reinforced hexagonal sandwich core structure had the maximum deflection. Compared to square

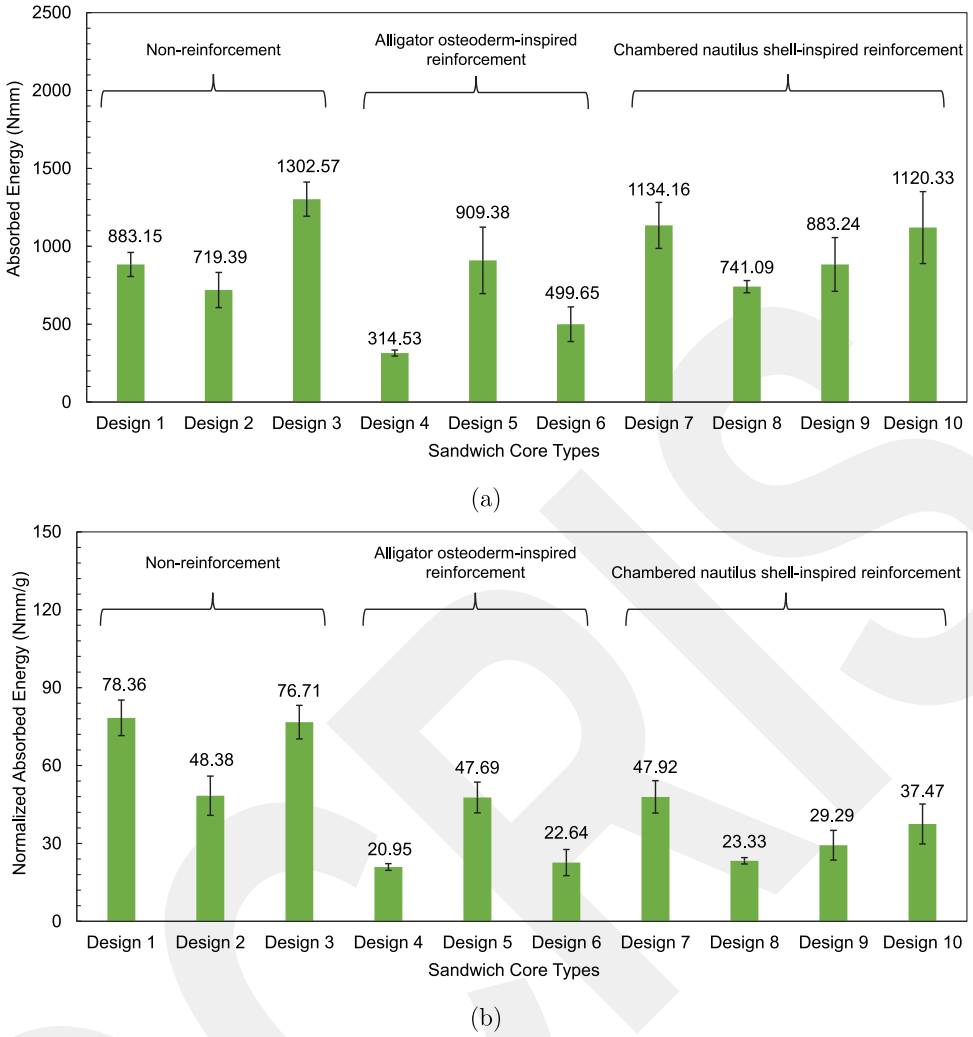

Fig. 10. Comparison of (a) measured and (b) normalized absorbed energy for different sandwich core types.

and circular outer cell designs, it was determined that the deformation ability of the hexagonal outer cell design was better under bending load. Design 8 had a normalized minimum deflection value. Although bio-inspired reinforcements significantly increased the load-carrying capacity of sandwich core structures, they reduced the deflection values of the sandwich core structures and caused the sandwich core structure to become more rigid.

4.3. Comparison of flexural stiffness

The measured and normalized flexural stiffness values of different sandwich core types are demonstrated in Fig. 9. Flexural stiffness is related to the damage-tolerant performance of sandwich core structures. Namely, high flexural stiffness provides high damage-tolerant performance. Sandwich core structures with high damage-tolerant performance are desired to obtain high-strength engineering structures. Flexural stiffness was calculated by the slope of the load–displacement curve in the elastic region (initial tangent modulus). Compared to chambered nautilus shell-inspired reinforcement, alligator osteoderm-inspired reinforcement significantly increased the flexural stiffness of sandwich core structures. According to normalized results, Design 4, with its hexagonal outer cell design and alligator osteoderm-inspired reinforcement, had the highest flexural stiffness. The damage-tolerant performance of the classical honeycomb structure was improved considerably with the alligator osteoderm-inspired reinforcement. Considering non-reinforced sandwich core structures, Design 2 with a square outer cell had the highest damage-tolerant performance, while Design 3 with a circular outer cell possessed the poorest damage tolerance performance. According to normalized test results of sandwich structures with the hexagonal outer cell (Designs 1, 4, 7), both bio-inspired reinforcements increased the flexural stiffness and the damage-tolerant performance of the classical honeycomb sandwich core structure. Considering the normalized test results of sandwich core structures with the square outer cell (Designs 2, 5, 8), alligator osteoderm-inspired reinforcement increased the

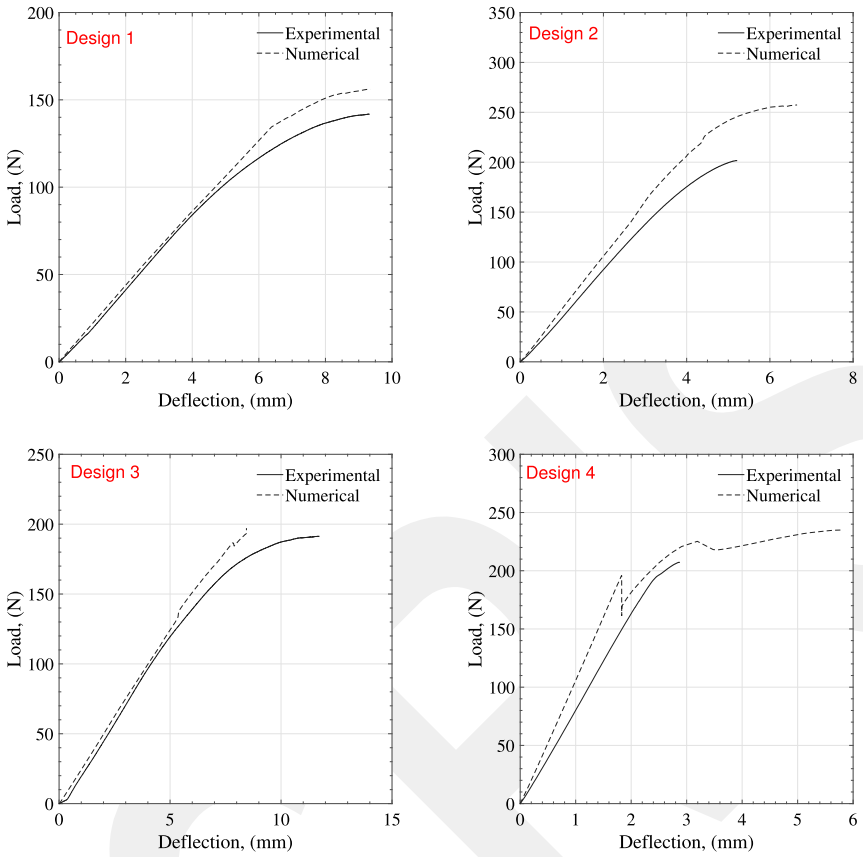

Fig. 11. Experimental and numerical load–deflection curves of the sandwich core designs.

flexural stiffness of sandwich core structures, while chambered nautilus shell-inspired reinforcement led to a decrease in the flexural stiffness and damage-tolerant performance. To sum up, according to measured flexural stiffness values, it was observed that both bio-inspired reinforcements increase the flexural stiffness and damage-tolerant performance of non-reinforced sandwich core structures. However, according to normalized results, the damage-tolerant performance of non-reinforced sandwich structures was significantly improved with the alligator osteoderm-inspired reinforcement for all outer cell designs (hexagonal, square, and circular).

4.4. Comparison of absorbed energy

Sandwich core structures with high energy absorption performance are desired in the manufacturing of lightweight and high-strength structures. Therefore, determining the effect of bio-inspired reinforcements on the energy absorption performance of sandwich core structures under bending load is crucial for industrial applications. Fig. 10 illustrates the measured and normalized absorbed energy of sandwich core structures. Among the non-reinforced sandwich core structures, Design 3 with the circular outer cell had the best energy absorption performance. The effect of reinforcement on the energy absorption performance of sandwich core structures was evaluated by considering sandwich core structures with similar outer cells. Considering Designs 1, 4, and 7, alligator osteoderm-inspired reinforcement decreased the energy absorption performance by increasing the flexural stiffness of the sandwich core structure, while chambered nautilus shell-inspired reinforcement improved the energy absorption performance of the honeycomb sandwich core structure. For square outer cell designs (Designs 2, 5, 8), alligator osteoderm-inspired reinforcement increased the energy absorption performance of sandwich core structures more than chambered nautilus shell-inspired reinforcement. Considering sandwich core structures with circular outer cells (Designs 3, 6, 9, 10), it was observed that bio-inspired reinforcements reduced the energy absorption capability of sandwich core structures under bending load. This is due to the fact that reinforcements reduced the deformation ability of sandwich core structures with the circular outer cell. According to weight-normalized absorbed energy results, considering non-reinforced sandwich core structures, Designs 1 and 3 had higher specific energy absorption capacity than Design 2. Both bio-inspired reinforcements reduced the specific energy absorption capacity of sandwich core structures due to reducing their deformation ability.

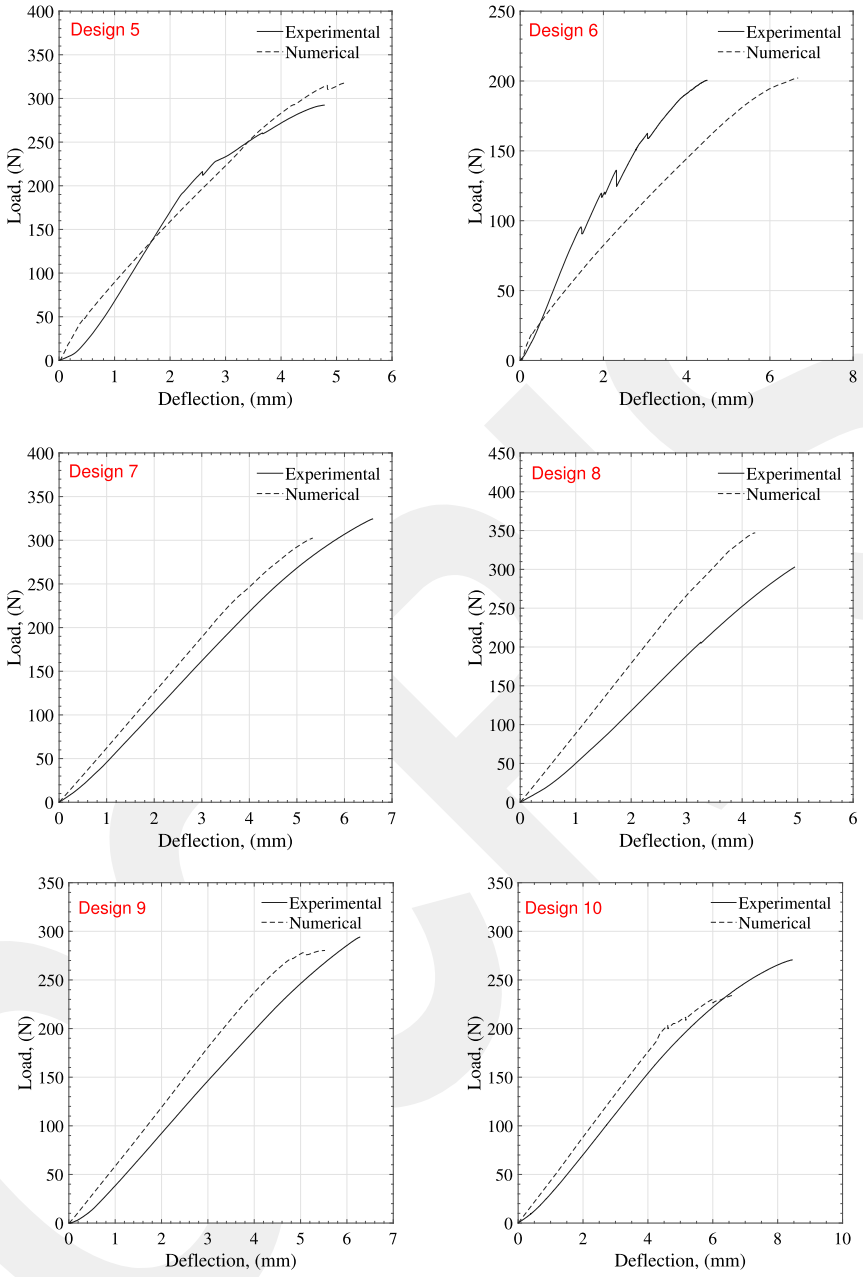

Fig. 11. (*continued*).

4.5. Damage analysis

Damage analysis of sandwich core structures under bending load was examined experimentally and numerically. The verification of the developed numerical model was performed by comparing experimental and numerical load–deflection curves. Fig. 11 illustrates the experimental and numerical load–displacement curves of sandwich core structures under bending load. In all sandwich core structures, after the load reached the maximum value, a sudden fracture occurred in the sandwich core structures and the sandwich core structures could not continue to carry the load. This is due to the mechanical properties of the PLA material used

in the production of the sandwich core material. Similar damage behavior was reported by Bru et al. [12]. Therefore, the curves in the load–deflection graphs of sandwich core structures covered up to the maximum load value, and the absorbed energy was calculated by taking into account the maximum load value and deflection values in the study performed by Bru et al. [12]. A similar approach was used in this study. Since sandwich core structures are completely damaged at the maximum load value, the load–deflection graph was presented up to the maximum load value. There is a generally good agreement between experimental and numerical results. The developed numerical model was able to successfully predict the bending behavior of sandwich core structures. The developed numerical model provides the determination of the damage types of sandwich core structures under bending load: compression, tension, and shear. According to the numerical analysis results, compression, tension, and shear damage types occurred in the sandwich core structures along the perpendicular to the raster orientation. Experimental and numerical damage images of sandwich core structures with a honeycomb outer cell are presented in Fig. 12. While the experimental damage images cover the sandwich core structure between the two bottom supports, the numerical damage images represent the middle of the sandwich core region where the bending moment is highest. The damage occurred close to the area where the bending load was applied (middle region) and the bending moment reached the highest value in this region. Damage was observed on the outer cell edges of the non-reinforced honeycomb sandwich core structure. Shear and tension damage types were more effective in the non-reinforced honeycomb sandwich core structure. Alligator osteoderm-inspired reinforcement prevented compression damage by increasing the damage-tolerant performance of the sandwich core structure, and instead of outer cell damage, the damage occurred only in the reinforcement. Tension and shear damage types were observed in alligator osteoderm-inspired reinforcement due to the buckling effect. In the sandwich core structure with the chambered nautilus shell-inspired reinforcement, damage occurred in the junction areas between the reinforcements and the outer cell edges. Compression and shear damage types were more dominant than tension damage.

Fig. 13 illustrates the damage types of sandwich core structures with the square outer cell. Non-reinforced and alligator osteoderm-inspired reinforced sandwich core structures resisted compressive stresses and therefore no compression damage occurred. While damage occurred at the outer cell edges in non-reinforced sandwich core structures, the reinforcements were damaged by the buckling effect for the sandwich core structures with the alligator osteoderm-inspired reinforcement. In sandwich core structures with the chambered nautilus shell-inspired reinforcement, damage was observed in the junction areas between the reinforcements and the outer cell edges. It was determined that tension and shear damage types were dominant modes in sandwich core structures with the square outer cell. Fig. 14 demonstrates the damage types of the sandwich core structures with the circular outer cell. In the non-reinforced sandwich core structure, damage occurred along the line where the bending moment was maximum. In the sandwich core structures with the alligator osteoderm-inspired and chambered nautilus shell-inspired reinforcements, the damage mostly occurred in the reinforcement structures. The failure of the overall structure occurred in all 3D-printed sandwich core structures under bending load. Local deformation regions were observed in bio-inspired reinforcements, however, the main damage type was based on the failure of the overall sandwich core structures.

The von Mises stress distributions in the sandwich core structures are shown in Fig. 15. Stress distribution images were obtained when damage initiated in the sandwich core structures. In non-reinforced sandwich core structures, the stress value decreased from the loading direction to the supports. The von Mises stress reached the highest value in the middle region where the bending moment was maximum. Alligator osteoderm-inspired and chambered nautilus shell-inspired reinforcements considerably changed the stress distributions of the sandwich core structures. The von Mises stress value reached higher levels in the reinforcement regions compared to the outer cell edges. Bio-inspired reinforcements played an effective role in carrying the bending load, reducing the stress value in the outer cells of the sandwich core structures, and preventing the outer cells from being damaged.

5. Conclusions

In this study, 3D-printed novel sandwich core designs with bio-inspired reinforcements were proposed. Their bending performances were comprehensively investigated by using experimental study and numerical analysis. The mechanical performances of sandwich core structures were compared, taking into account load-carrying capacity, largest deflection, flexural stiffness (damage-tolerant capability), energy absorption performance, and damage mode. The main results were presented as follows:

- Considering non-reinforced sandwich core structures, Design 2 (square outer cell) showed the highest load-carrying capacity performance. According to the normalized test results, alligator osteoderm-inspired reinforcement improved the load-carrying capacity performance of the sandwich core structure. However, it reduced the deformation capability of the sandwich core structures.
- Alligator osteoderm-inspired reinforcement significantly enhanced the damage-tolerant performance of sandwich core structures compared to chambered nautilus shell-inspired reinforcement.
- As reinforcements reduced the deformation capability of sandwich core structures, both bio-inspired reinforcements decreased the specific energy absorption capacity of sandwich core structures. However, Designs 5 and 8 showed better energy absorption performance than non-reinforced sandwich core structures.
- Bio-inspired reinforcements considerably affected the stress distribution and damage behavior of the sandwich core structures for all outer cell types (hexagon, square, circular). They reduced the von Mises stress level of the outer cell edges, resulting in reinforcement damage instead of outer cell damage.

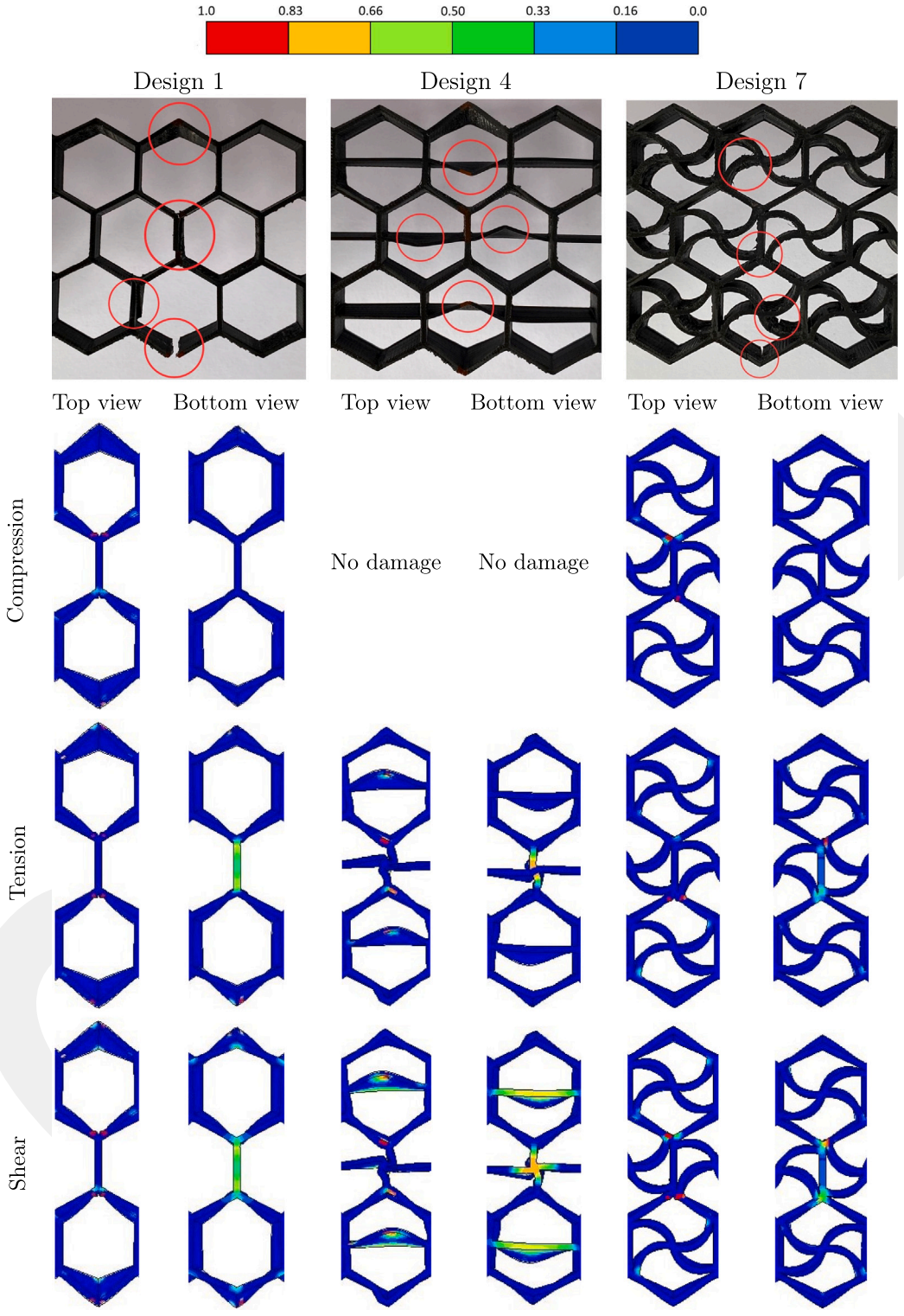

Fig. 12. Damage types of the sandwich core structures with the honeycomb outer cell.

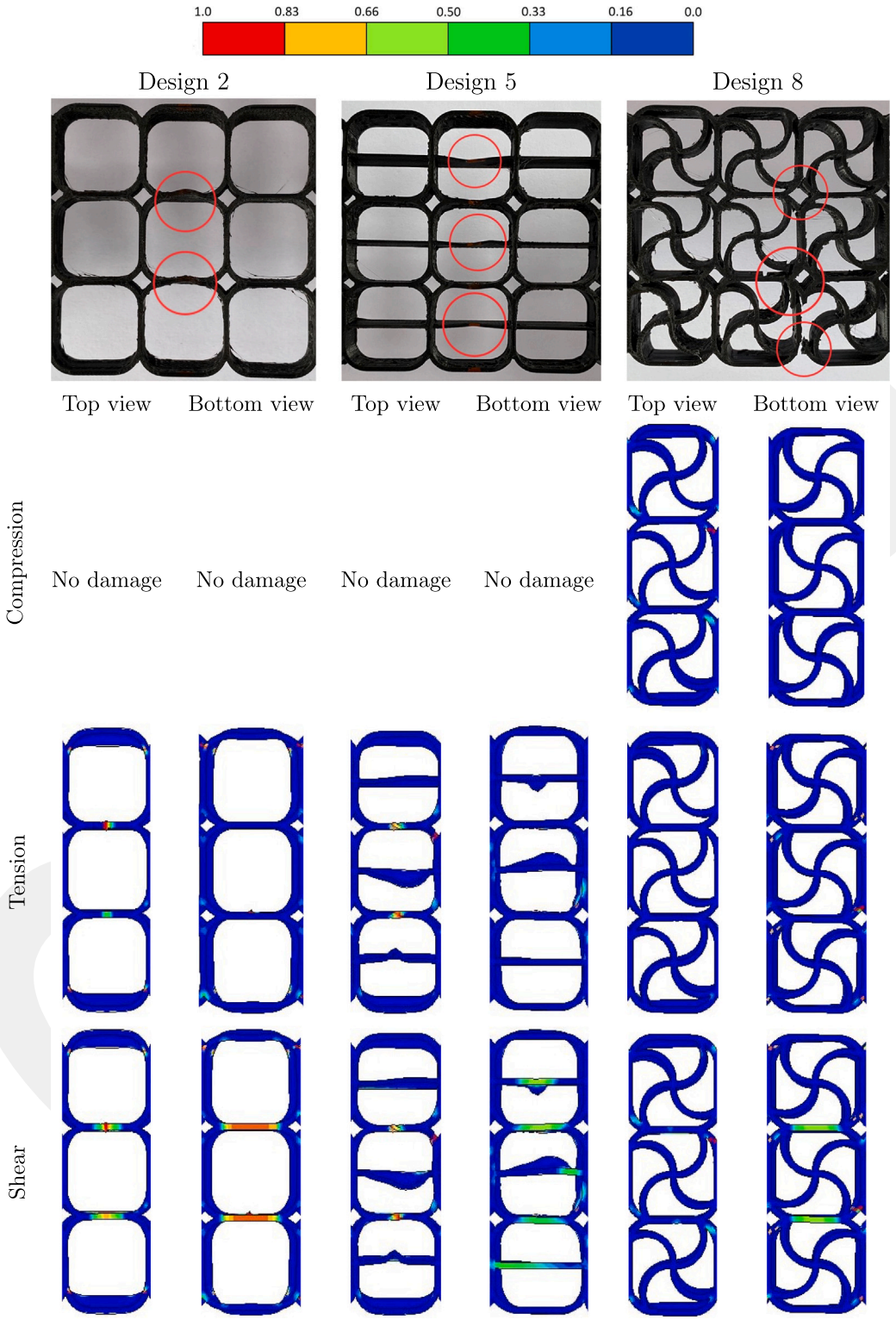

Fig. 13. Damage types of the sandwich core structures with the square outer cell.

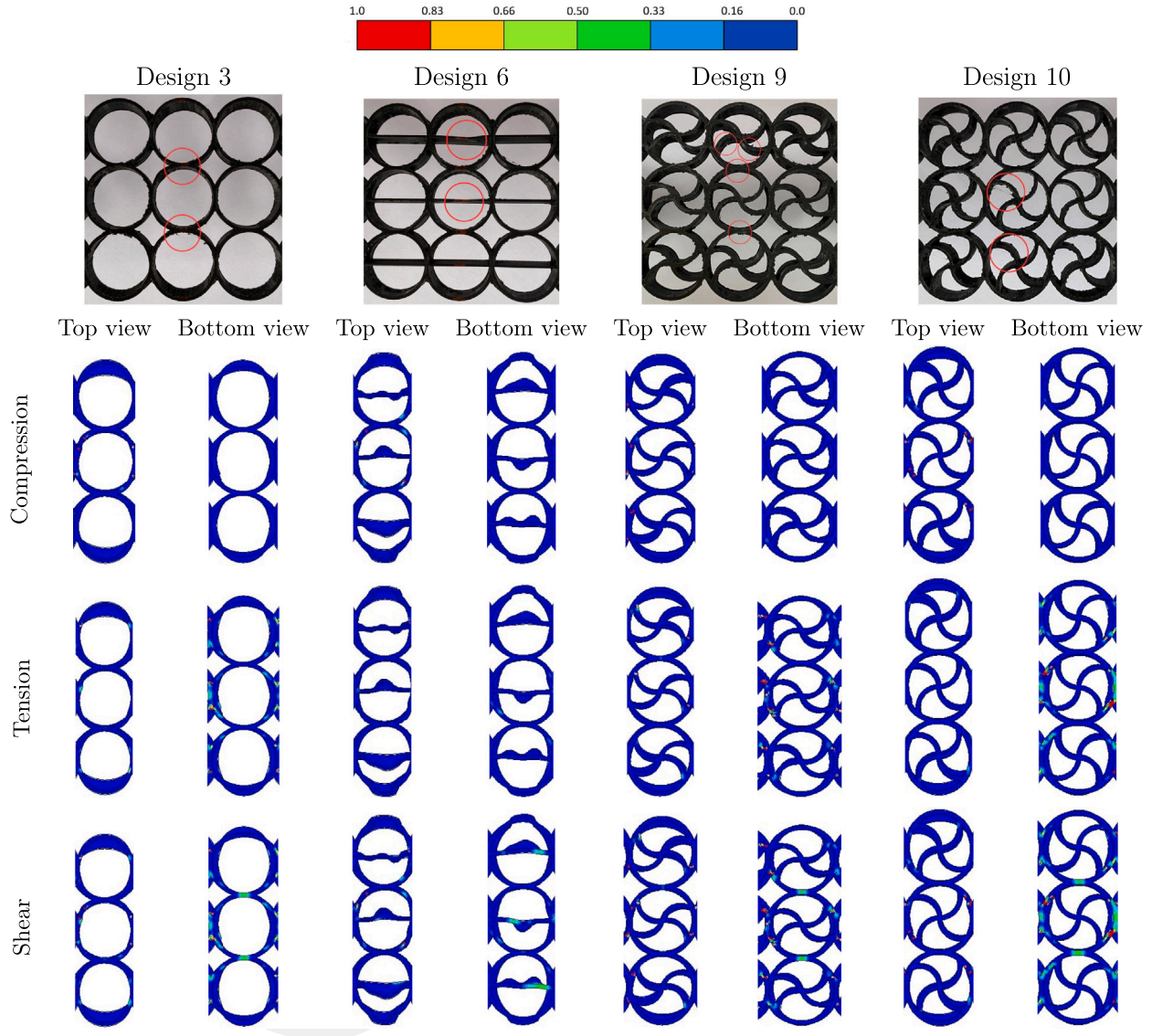

Fig. 14. Damage types of the sandwich core structures with the circular outer cell.

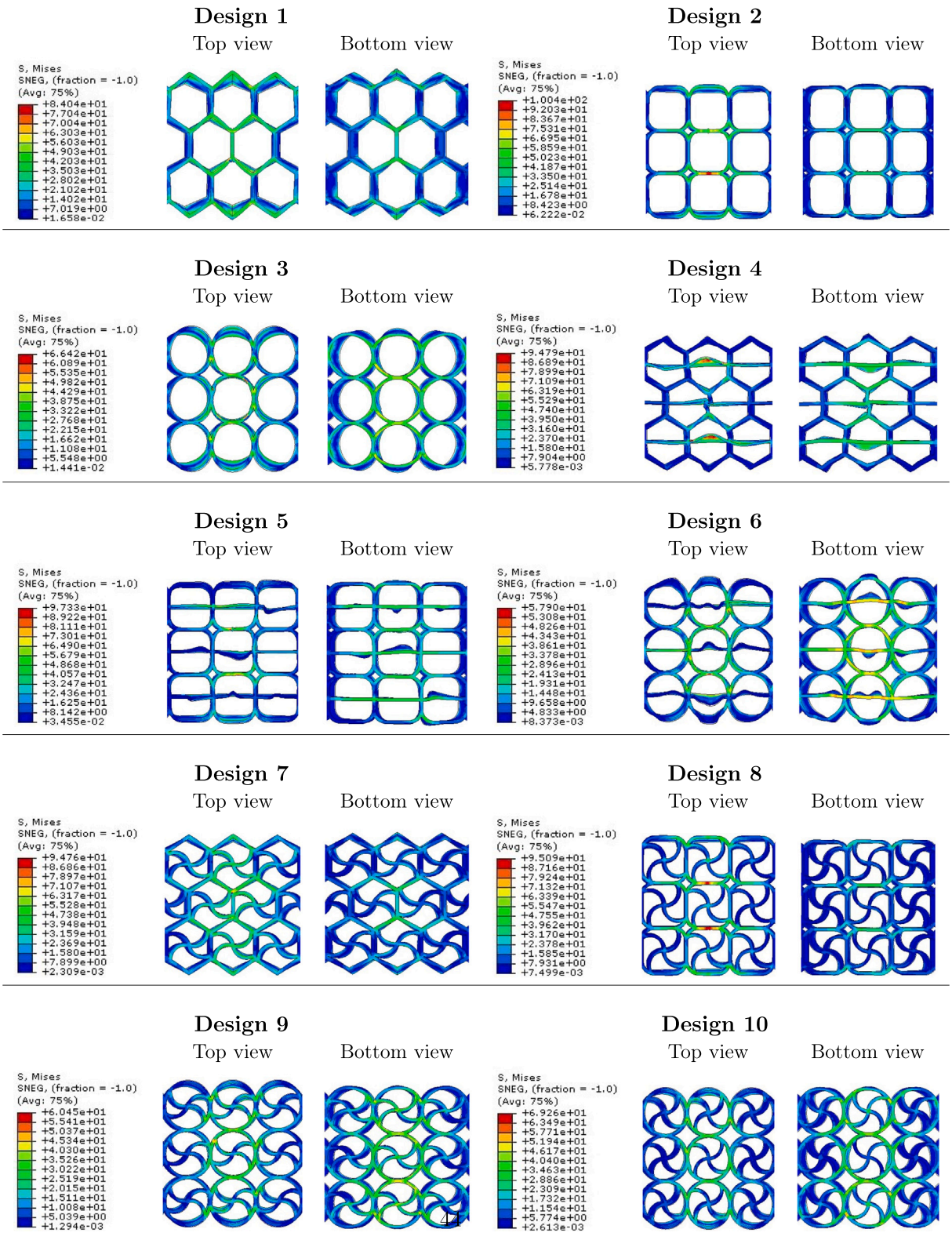

Fig. 15. Stress distributions in the non-reinforced and reinforced sandwich core structures.

CRediT authorship contribution statement

M. Gokhan Atahan: Writing – review & editing, Writing – original draft, Visualization, Supervision, Software, Project administration, Methodology, Conceptualization. **Merve Erikli:** Visualization, Resources, Project administration, Investigation, Formal analysis, Conceptualization. **Enes Ozipek:** Visualization, Resources, Investigation, Formal analysis. **Fulya Ozgun:** Visualization, Resources, Investigation.

Declaration of competing interest

The authors declare that they have no known competing financial interests or personal relationships that could have appeared to influence the work reported in this paper.

Data availability

Data will be made available on request.

Acknowledgments

This research was financially supported by the Scientific and Technological Research Council of Türkiye (TÜBİTAK-2209A: Project number 1919B012205643).

References

[1] V. Birman, G.A. Kardomateas, Review of current trends in research and applications of sandwich structures, Composites B 142 (2018) 221–240.
[2] R. Azadi, M.H. Pashaei, H. Gorji, M. Bakhshi Jooybari, Y. Rostamiyan, Experimental and statistical investigation of the three-point bending strength of the composite sandwich beams with trapezoidal core, J. Compos. Mater. 56 (30) (2022) 4675–4692.
[3] C. Qi, F. Jiang, S. Yang, Advanced honeycomb designs for improving mechanical properties: A review, Composites B 227 (2021) 109393.
[4] X. Zhao, L. Wei, D. Wen, G. Zhu, Q. Yu, Z. Ma, Bending response and energy absorption of sandwich beams with novel auxetic honeycomb core, Eng. Struct. 247 (2021) 113204.
[5] Z. Liu, H. Chen, S. Xing, Mechanical performances of metal-polymer sandwich structures with 3D-printed lattice cores subjected to bending load, Arch. Civ. Mech. Eng. 20 (2020) 1–17.
[6] G. Sun, X. Huo, D. Chen, Q. Li, Experimental and numerical study on honeycomb sandwich panels under bending and in-panel compression, Mater. Des. 133 (2017) 154–168.
[7] Y. Sun, L.-c. Guo, T.-s. Wang, S.-y. Zhong, H.-z. Pan, Bending behavior of composite sandwich structures with graded corrugated truss cores, Compos. Struct. 185 (2018) 446–454.
[8] M. Rangapuram, S. Dasari, J.W. Newkirk, K. Chandrashekhara, H. Misak, P. Toivonen, D. Klenosky, T. Unruh, J. Sam, Performance evaluation of composite sandwich structures with additively manufactured aluminum honeycomb cores with increased bonding surface area, Polym. Compos. 44 (9) (2023) 5357–5368.
[9] S. Chahardoli, Flexural behavior of sandwich panels with 3D printed cellular cores and aluminum face sheets under quasi-static loading, J. Sandw. Struct. Mater. 25 (2) (2023) 232–250.
[10] A.I. Indreş, D.M. Constantinescu, O.A. Mocian, Bending behavior of 3D printed sandwich beams with different core topologies, Mater. Des. Process. Commun. 3 (4) (2021) e252.
[11] A. Haldar, V. Managuli, R. Munshi, R. Agarwal, Z. Guan, Compressive behaviour of 3D printed sandwich structures based on corrugated core design, Mater. Today Commun. 26 (2021) 101725.
[12] J. Bru, M. Leite, A. Ribeiro, L. Reis, A. Deus, M. Fátima Vaz, Bioinspired structures for core sandwich composites produced by fused deposition modelling, Proc. Inst. Mech. Eng., Part L: J. Mater.: Des. Appl. 234 (3) (2020) 379–393.
[13] C. Lu, M. Qi, S. Islam, P. Chen, S. Gao, Y. Xu, X. Yang, Mechanical performance of 3D-printing plastic honeycomb sandwich structure, Int. J. Precis. Eng. Manuf.-Green Technol. 5 (2018) 47–54.
[14] T. Li, L. Wang, Bending behavior of sandwich composite structures with tunable 3D-printed core materials, Compos. Struct. 175 (2017) 46–57.
[15] H. Geramizadeh, S. Dariushi, S.J. Salami, Numerical and experimental investigation for enhancing the energy absorption capacity of the novel three-dimensional printed sandwich structures, Proc. Inst. Mech. Eng., Part L: J. Mater.: Des. Appl. 235 (7) (2021) 1622–1634.
[16] S. Pirouzfar, A. Zeinedini, Effect of geometrical parameters on the flexural properties of sandwich structures with 3D-printed honeycomb core and E-glass/epoxy face-sheets, Structures 33 (2021) 2724–2738.
[17] H. Geramizadeh, S. Dariushi, S.J. Salami, Optimal face sheet thickness of 3D printed polymeric hexagonal and re-entrant honeycomb sandwich beams subjected to three-point bending, Compos. Struct. 291 (2022) 115618.
[18] M. Eryildiz, Experimental investigation and simulation of 3D printed sandwich structures with novel core topologies under bending loads, Int. Polym. Process. 38 (3) (2023) 277–289.
[19] X. Zhang, C. Xu, W. Li, Z. Su, Study on the bending and shear properties of quasi-honeycomb sandwich structures considering the variable-density core design, Compos. Struct. (2023) 117517.
[20] N.S. Ha, G. Lu, X. Xiang, Energy absorption of a bio-inspired honeycomb sandwich panel, J. Mater. Sci. 54 (2019) 6286–6300.
[21] N. San Ha, G. Lu, A review of recent research on bio-inspired structures and materials for energy absorption applications, Composites B 181 (2020) 107496.
[22] W. Zhang, J. Xu, T. Yu, Dynamic behaviors of bio-inspired structures: Design, mechanisms, and models, Eng. Struct. 265 (2022) 114490.
[23] S.A. Sabah, A. Kueh, M. Al-Fasih, Comparative low-velocity impact behavior of bio-inspired and conventional sandwich composite beams, Compos. Sci. Technol. 149 (2017) 64–74.
[24] A. Sethi, P. Budarapu, V. Vusa, Nature-inspired bamboo-spiderweb hybrid cellular structures for impact applications, Compos. Struct. 304 (2023) 116298.
[25] Q.-W. Li, B.-H. Sun, Numerical analysis of low-speed impact response of sandwich panels with bio-inspired diagonal-enhanced square honeycomb core, Int. J. Impact Eng. 173 (2023) 104430.
[26] X. Yu, L. Pan, J. Chen, X. Zhang, P. Wei, Experimental and numerical study on the energy absorption abilities of trabecular–honeycomb biomimetic structures inspired by beetle elytra, J. Mater. Sci. 54 (3) (2019) 2193–2204.

[27] G. Chouhan, B.M. Gunji, P. Bidare, D. Ramakrishna, R. Kumar, Experimental and numerical investigation of 3D printed bio-inspired lattice structures for mechanical behaviour under quasi static loading conditions, Mater. Today Commun. 35 (2023) 105658.
[28] C. Bhat, A. Kumar, S.-C. Lin, J.-Y. Jeng, A novel bioinspired architectured materials with interlocking designs based on tessellation, Addit. Manuf. 58 (2022) 103052.
[29] R. Doodi, B.M. Gunji, An experimental and numerical investigation on the performance of novel hybrid bio-inspired 3D printed lattice structures for stiffness and energy absorption applications, Mech. Adv. Mater. Struct. (2023) 1–10.
[30] C. Peng, K. Fox, M. Qian, H. Nguyen-Xuan, P. Tran, 3D printed sandwich beams with bioinspired cores: Mechanical performance and modelling, Thin-Walled Struct. 161 (2021) 107471.
[31] K. Song, D. Li, C. Zhang, T. Liu, Y. Tang, Y.M. Xie, W. Liao, Bio-inspired hierarchical honeycomb metastructures with superior mechanical properties, Compos. Struct. 304 (2023) 116452.
[32] I. Ullah, J. Elambasseril, M. Brandt, S. Feih, Performance of bio-inspired kagome truss core structures under compression and shear loading, Compos. Struct. 118 (2014) 294–302.
[33] Z. Hu, K. Thiyagarajan, A. Bhusal, T. Letcher, Q.H. Fan, Q. Liu, D. Salem, Design of ultra-lightweight and high-strength cellular structural composites inspired by biomimetics, Composites B 121 (2017) 108–121.
[34] Y. Nian, S. Wan, X. Li, Q. Su, M. Li, How does bio-inspired graded honeycomb filler affect energy absorption characteristics? Thin-Walled Struct. 144 (2019) 106269.
[35] Y. Zhang, M. Lu, C.H. Wang, G. Sun, G. Li, Out-of-plane crashworthiness of bio-inspired self-similar regular hierarchical honeycombs, Compos. Struct. 144 (2016) 1–13.
[36] X. Yang, J. Ma, Y. Shi, Y. Sun, J. Yang, Crashworthiness investigation of the bio-inspired bi-directionally corrugated core sandwich panel under quasi-static crushing load, Mater. Des. 135 (2017) 275–290.
[37] S. Song, C. Xiong, J. Yin, Y. Qin, H. Deng, K. Cui, Failure mechanism and size effect of new bioinspired sandwich under quasi-static load, Compos. Struct. (2023) 117552.
[38] C.-Y. Sun, P.-Y. Chen, Structural design and mechanical behavior of alligator (Alligator mississippiensis) osteoderms, Acta Biomater. 9 (11) (2013) 9049–9064.
[39] A.S. Perera, M.-O. Coppens, Re-designing materials for biomedical applications: from biomimicry to nature-inspired chemical engineering, Phil. Trans. R. Soc. A 377 (2138) (2019) 20180268.
[40] T.M. Scheyer, P.M. Sander, Histology of ankylosaur osteoderms: implications for systematics and function, J. Vert. Paleontol. 24 (4) (2004) 874–893.
[41] ASTM C393/C393M-20, standard test method for core shear properties of sandwich constructions by beam flexure.
[42] S. Kazemahvazi, D. Tanner, D. Zenkert, Corrugated all-composite sandwich structures. Part 2: Failure mechanisms and experimental programme, Compos. Sci. Technol. 69 (7–8) (2009) 920–925.
[43] A.W. Alshaer, D.J. Harland, An investigation of the strength and stiffness of weight-saving sandwich beams with CFRP face sheets and seven 3D printed cores, Compos. Struct. 257 (2021) 113391.
[44] M. Anoop, P. Senthil, Homogenisation of elastic properties in FDM components using microscale RVE numerical analysis, J. Brazil. Soc. Mech. Sci. Eng. 41 (12) (2019) 1–16.
[45] R. Torre, S. Brischetto, Experimental characterization and finite element validation of orthotropic 3D-printed polymeric parts, Int. J. Mech. Sci. 219 (2022) 107095.
[46] A. Sabik, M. Rucka, A. Andrzejewska, E. Wojtczak, Tensile failure study of 3D printed PLA using DIC technique and FEM analysis, Mech. Mater. 175 (2022) 104506.
[47] ABAQUS, Analysis User's Guide Documentation Version 6.13, Dassault Systems SIMULIA Corp, 2013.
[48] A. Matzenmiller, J. Lubliner, R. Taylor, A constitutive model for anisotropic damage in fiber-composites, Mech. Mater. 20 (1995) 125–152.
[49] Z. Hashin, A. Rotem, A fatigue failure criterion for fiber reinforced materials, J. Compos. Mater. 7 (4) (1973) 448–464.
[50] Z. Hashin, Failure criteria for unidirectional fiber composites, J. Appl. Mech. 47 (1980) 329–334.
[51] P.P. Camanho, C.G. Dávila, Mixed-mode decohesion finite elements for the simulation of delamination in composite materials, NASA/TM-2002-211737 (2002) 1–37.
[52] M.G. Atahan, M.K. Apalak, Loading-rate effect on tensile and bending strength of 3D-printed polylactic acid adhesively bonded joints, J. Adhes. Sci. Technol. 36 (3) (2022) 317–344.
[53] Y. Song, Y. Li, W. Song, K. Yee, K.-Y. Lee, V.L. Tagarielli, Measurements of the mechanical response of unidirectional 3D-printed PLA, Mater. Des. 123 (2017) 154–164.
[54] S.R. Rajpurohit, H.K. Dave, Impact strength of 3D printed PLA using open source FFF-based 3D printer, Prog. Addit. Manuf. 6 (1) (2021) 119–131.